Journal of Chromatography A, 1218 (2011) 3763–3770

Contents lists available at ScienceDirect

Journal of Chromatography A

journal homepage: www.elsevier.com/locate/chroma

# Novel molecularly imprinted microsphere using a single chiral monomer and chirality-matching (S)-ketoprofen template

Jiabing Jiang[a], Kesheng Song[b], Zhi Chen[a], Qi Zhou[a], Youwen Tang[a,*], Fenglong Gu[b,*], Xiongjun Zuo[a], Zhiguang Xu[a]

[a] Department of Chemistry, South China Normal University, Guangzhou 510006, China
[b] Center for Computational Quantum Chemistry, South China Normal University, Guangzhou 510006, China

ARTICLE INFO

*Article history:*
Received 3 December 2010
Received in revised form 14 April 2011
Accepted 16 April 2011
Available online 27 April 2011

*Keywords:*
Surface molecular imprinting technique
Synergistic effect
Enantiomer separation
Ketoprofen
High-performance liquid chromatography
Computational simulation

ABSTRACT

We designed and synthesized a cinchonine derivative to be used as a novel chiral monomer. It was employed in a dual role of functional monomer and cross-linking monomer, displaying multi-binding sites for the template (S)-ketoprofen. Monodisperse molecularly imprinted core-shell microspheres were prepared using surface imprinting method on silica gel. The results show a substantial synergistic effect in the enantioselective recognition, confirming our initial hypothesis. Computational simulation of the monomer and template pre-arrangement strongly supports our proposed chiral recognition mechanism for the imprinted microspheres.



## 1. Introduction

Molecular imprinting is a technique for creation of polymeric matrices containing tailor-made receptors with specific molecular recognition ability [1]. During the first step of the process, polymerizable functional monomers are arranged around a template molecule and co-polymerized with crosslinking monomers. The template is then extracted from the resulting polymer, generating target-specific binding cavities which are complementary to the template in size, shape and functional groups [2]. Molecularly imprinted polymers (MIPs) show high selectivity and affinity towards the template. Because of their outstanding molecular recognition characteristics, MIPs have drawn much attention in various fields, such as drug delivery [3–7], solid-phase extractions [8–12], chromatographic separations [13–15], biomimetic sensing [16–18] and mimic enzyme catalysis [19,20]. MIPs have been researched for many years for the purpose of chiral separation; they are exploited as chiral stationary phase in separation of a broad range of chiral compounds, such as amino acidic derivatives [21–23], peptides [24,25] and various pharmaceutical drugs [26–28]. The available data demonstrate that the concept of imprinting is highly suitable for developing robust artificial receptors with chiral recognition properties; such receptors can be utilized in detection and separation of many different compounds and their analogues.

The choice of functional monomer is very important for the chiral separation selectivity of MIPs. Currently, the most commonly used functional monomers are acrylamide, methacrylic acid and 4-vinyl pyridine. These monomers have limited ability for molecular recognition [29], particularly in case of chiral compounds. Recently, Gavioli et al. [30] have used cinchona alkaloid derivative as functional monomer and successfully prepared 3, 5-dichlorobenzoyl amino acid imprinted polymers with a high template retention factor.

Existing molecular imprinting techniques employ mainly single enantiomer template molecules and non-chiral functional monomers to predetermine chiral three-dimensional cavities and prepare chiral MIPs for enantioselective recognition applications. The traditional chiral stationary phases (CSPs) in liquid chromatography, such as cellulose, amylase and cyclodextrin, are used to investigate the resolution ability of chiral selectors.

This work focuses on creation of novel molecularly imprinted microspheres (MIMs) using a single chiral monomer, and investigates the synergistic effect between chiral monomer and chiral

* Corresponding authors. Tel.: +86 20 39310369.
*E-mail address:* tanglab@scnu.edu.cn (Y. Tang).

0021-9673/$ – see front matter © 2011 Elsevier B.V. All rights reserved.
doi:10.1016/j.chroma.2011.04.043

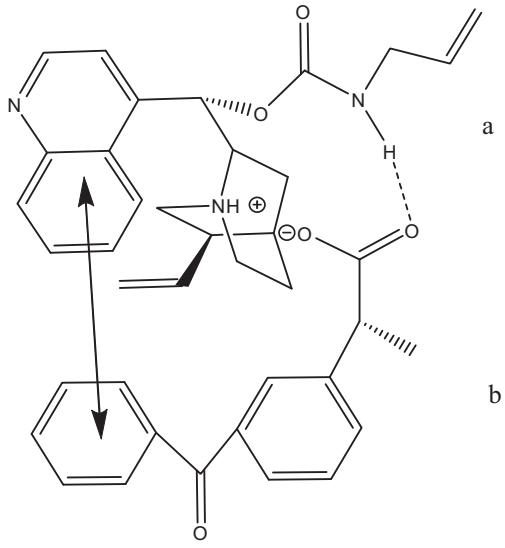


**Fig. 1.** The pre-arrangement between chiral monomer (a) and (S)-ketoprofen (b).

cavity in enantioselective recognition. We selected (S)-ketoprofen, a typical non-steroidal anti-inflammatory drug, as the template molecule. Taking into account its chemical structure, we designed and synthesized a new polymerizable cinchonine derivative. It was used as a single chiral monomer, playing a dual role of functional monomer and cross-linker. We postulate that this chiral monomer might have (S)-ketoprofen multi-binding sites (Fig. 1); this assumption is strongly supported by the results of our computational simulation.

## 2. Experimental

### 2.1. Chemicals and instruments

We made silica particles (diameter about 5 μm) [31] and used them as the support medium to prepare the (S)-ketoprofen (KEP) imprinted microspheres. (S)-ketoprofen and rac-ketoprofen were purchased from Hubei Anlian Pharmaceutical Factory (Wuhan, China). Rac-ibuprofen (IBU) was kindly provided by Suzhou No. 4 Pharmaceutical Factory (Suzhou, China). Rac-naproxen (NAP) was purchased from ShanghaiDingxin Science and Technology Corporation (Shanghai, China). Cinchonine, quinidine, allyl isocyanate, dibutytin dilaurate, 3-methacryloyloxypropyltrimethoxysilane (MPTS) and 2,2′-azobisisobutyronitrile (AIBN) were from Alfa Aesar (Tianjin, China). Toluene, trichloromethane, acetic acid and methanol were from Kermel (Tianjin, China). All chemical reagents were of analytical or HPLC grade.

FT-IR spectra were recorded using a PE Spectrum One FT-IR Spectrometer from PerkinElmer (Foster City, CA, USA). NMR spectra were obtained on a Bruker Vector33 400 MHz spectrometer (Bremen, Germany). The morphology of the MIMs was investigated using a Philips XL-30 scanning electron microscope (Eindhoven, Holland). The HPLC utilized a Shimadzu LC-10AD pump, and a Shimadzu SPD-10A UV/Vis detector was obtained from Shimadzu Company (Kyoto, Japan).

### 2.2. Preparation of (S)-ketoprofen imprinted core-shell microspheres

#### 2.2.1. Silica-based supports

The silica microsphere surface was activated using the previously described method [32]. 10.0 g of silica microspheres was stirred into 250 mL of aqueous solution containing 8 mol/L hydrochloric acid and refluxed at 80 °C for 8 h. The solid product was recovered by filtration. It was washed with distilled water to neutralize it and dried under vacuum, at 120 °C for 12 h. 10.0 g of activated silica microspheres was mixed into 110 mL dry toluene-pyridine solution (10:1, v/v), and then 10.0 mL of MPTS was added to the mixture. The suspension was heated at 110 °C for 24 h, under nitrogen protection. The silica microspheres were collected and washed several times, successively, with toluene, methanol, distilled water and acetone. Finally, the vinylated silica microspheres were dried under vacuum at 80 °C for 6 h and used for the immobilization of the polymer. The activation process is shown in Fig. 2a.

**Table 1**
The preparative composition of different polymers.

| Polymers | (S)-ketoprofen (mmol) | ACC (mmol) | ACQ (mmol) | AIBN (g) |
|---|---|---|---|---|
| MIM1 | 1.19 | 2.38 | – | 0.10 |
| MIM2 | 2.38 | 2.38 | – | 0.10 |
| MIM3 | 4.72 | 2.38 | – | 0.10 |
| MIM4 | 7.14 | 2.38 | – | 0.10 |
| MIM5 | 4.72 | – | 2.38 | 0.10 |
| NIMs | – | 2.38 | – | 0.10 |

#### 2.2.2. Synthesis of the monomers

The synthesis of allylcarbamate-cinchonine ester (ACC) was performed following the procedure shown in Fig. 2b [33]. 3.0 g of cinchonine was dissolved in 200 mL of dry chloroform, with addition of 0.9 mL of allyl isocyanate, and 1 drop of dibutyltin dilaurate as a catalyst. The mixture was refluxed for 8 h, the solvent evaporated and the remaining raw material washed with n-hexane. The yellowish solid, allylcarbamate-cinchonine ester, was crystallized in chloroform/cyclohexane (procedure's yield: 80%). Physical properties of ACC were: m.p.: 195–197 °C; IR peak (KBr)/$cm^{-1}$: 3306, 2934, 2859, 1719, 1507. $^1$H NMR (TMS, $C_2D_6SO$): 8.85(d, 1H), 8.25(d, 1H), 8.01(s, 1H), 7.65(d,1H), 7.59(d,1H), 7.50(s,1H), 6.45(d,1H), 6.05(m,1H), 5.69(m,1H), 5.07(dd,4H), 3.51(d,2H), 3.26(d,1H), 2.61(m,2H), 2.22–0.86(m,9H). ESI-MS *m/z* calculated for $C_{23}H_{27}N_3O_2$ (M+1) was 378.21, the measured value was 378.34. The allylcarbamate-quinidine ester (ACQ) was synthesized in the same manner, except that quinidine was used instead of cinchonine. Physical properties of ACQ were: m.p.: 165–167 °C; IR peak (KBr)/$cm^{-1}$: 3356, 3067, 2934, 2871, 1711, 1513. $^1$H NMR (TMS, $CDCl_3$): 8.73(d,1H), 8.00(d, 1H), 7.36(d, 2H), 7.35 (s,1H), 6.48(d,1H), 5.84(m,1H), 5.79(m,1H), 5.11(d,4H), 3.95(s,3H), 3.80(d,2H), 3.28(m,1H), 2.97(d,2H), 2.76(m,2H), 2.26–1.56(m,6H); ESI-MS *m/z* calculated for $C_{24}H_{29}N_3O_3$ (M+1) was 408.22, the measured value was 408.30.

#### 2.2.3. Immobilization of MIPs on vinylated silica microspheres

A series of molecularly imprinted core-shell microspheres was prepared in chloroform, using the ingredients' amounts presented in Table 1. In a typical experiment procedure (Fig. 2c), an appropriate amount of (S)-ketoprofen was dissolved in 200 mL chloroform, and then 2.0 g of vinylated silica microspheres was dispersed in the solution. 1.2 g of ACC was added, stirring continuously. The polymerization was started by adding AIBN (0.10 g) under $N_2$ protection, at 60 °C, and the mixture was left to react, stirred continuously, for 18 h. The solids were collected and washed, successively, with chloroform, distilled water and methanol. At this point, the silica microsphere surface was grafted with the molecularly imprinted polymers.

As a control, non-imprinted microspheres (NIMs) were prepared following the same procedure, except for the absence of the template.

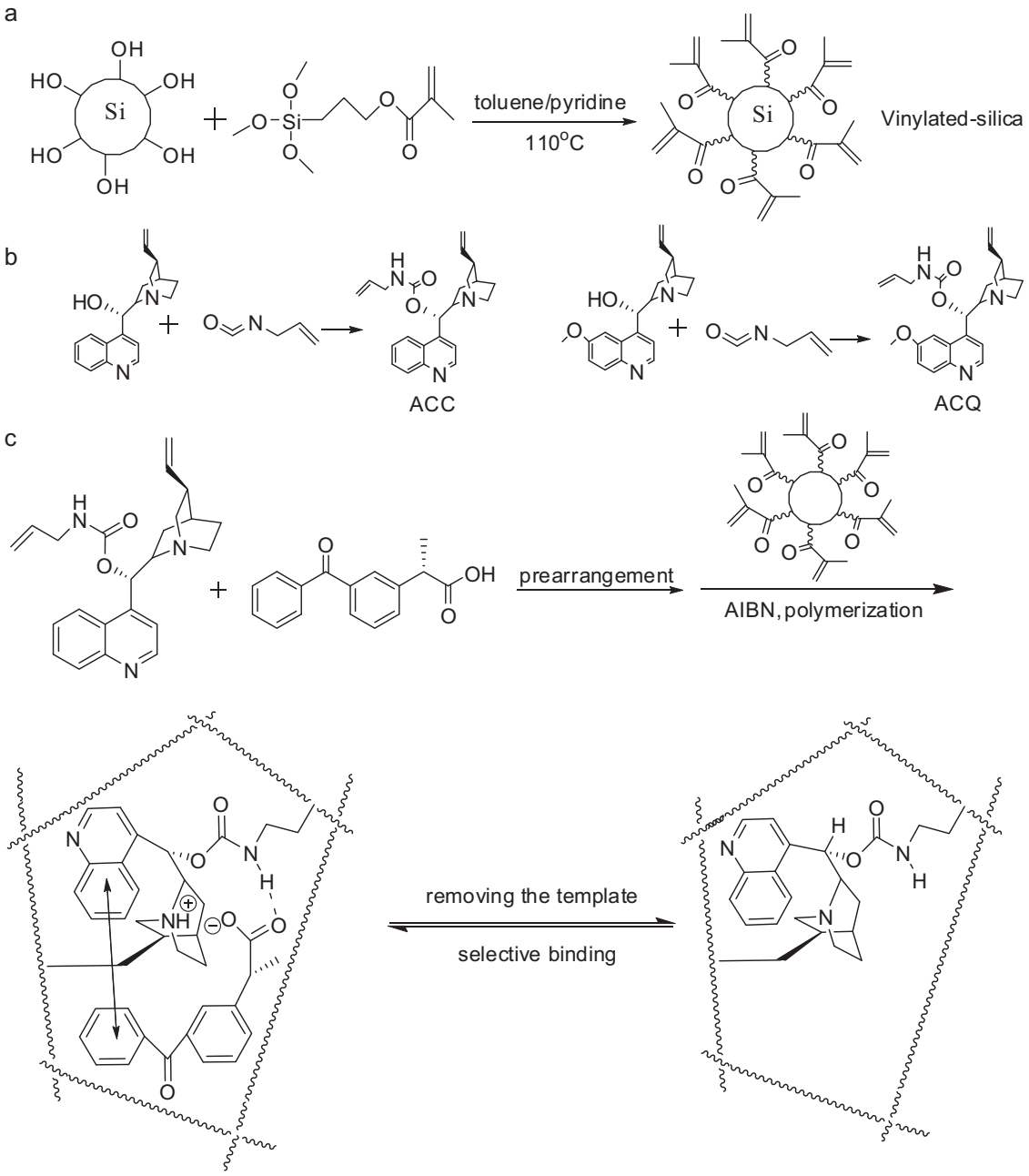


**Fig. 2.** Preparation of MIMs. (a) Synthesis of vinylated silica microspheres; (b) synthesis of the chiral monomer; (c) immobilization of MIPs on vinylated silica microspheres.

### 2.3. HPLC experiments

2.0 g aliquots of MIMs (or NIMs) were packed into stainless-steel columns (150 mm × 4.6 mm) using a conventional slurry method. The residual template and chiral monomer were completely eluted with a mobile-phase consisting of acetic acid-methanol mixture (5:95, v/v), at 0.4 mL/min, until a stable baseline was obtained. The UV detection wavelength was set at 265 nm. The mobile phase consisted of methanol-ammonium acetate (0.01 mol/L, pH = 3.5) with a volume ratio of 80:20. The flow rate of the mobile phase was 0.4 mL/min. 5 μL of 0.2 mmol/L of (S)-ketoprofen was injected for analysis. All the HPLC experiments were carried out at 25 °C. Retention behavior of the analyte was estimated using capacity factor ($\kappa$), calculated according to the equation

$$\kappa = \frac{t_1 - t_0}{t_0}$$

where $t_1$ and $t_0$ were the retention times of the analyte and unretained solute, respectively. Resolution was calculated according to the equation

$$R = \frac{2(t_S - t_R)}{W_S + W_R}$$

where $t_S$ and $t_R$ are the retention times of the (S)-isomer and (R)-isomer, respectively, and $W$ is the width, at the baseline, between tangents drawn to the inflection points of the peak.

### 2.4. Computational simulation

The energies of KEP, NAP and IBU, the functional monomer and the complex were calculated with the Gaussian 03 software package [34]. Their molecular geometries were optimized using B3LYP/6-31g (d, p) [35,36]. Additional, vibrational frequency calcu-

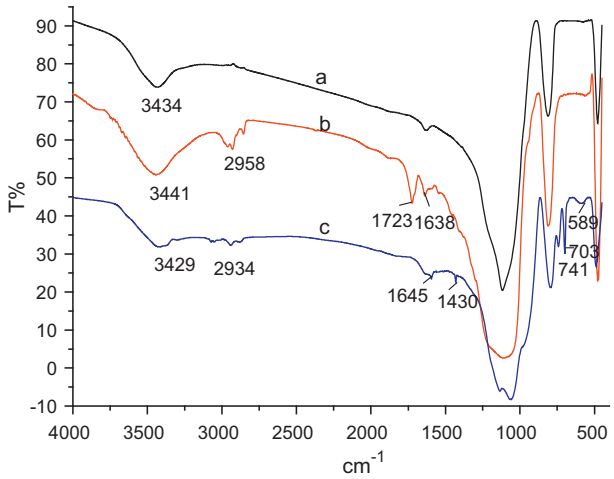


**Fig. 3.** FT-IR spectra of the activated silica gel (a), vinylated silica gel (b) and MIM3 (c).

lations at the same level of theory were performed to determine if the stationary points were local minima (zero imaginary frequency) and obtain zero-point energy corrections. Solvent effects were estimated using the polarizable continuum model (PCM) [37–39] with $CHCl_3$ as the solvent. The binding energies ($\Delta E$) of complex between chiral monomer and template or its analogues evaluated by the following equation:

$$\Delta E = E(\text{complex}) - E(\text{functional monomer}) - E(\text{template or analogue})$$

### 2.5. Binding experiments

The mixture of methanol and water (10:90, v/v) was used as the adsorption solvent. 20.0 mg of dried MIM3 or NIMs was added to 10 mL conical flasks containing 2.0 mL of (S)-ketoprofen of various initial concentrations. The flasks were shaken at 30 °C for 24 h. After that, the MIM3 or NIMs were isolated and the residual concentration of (S)-ketoprofen in solution was established using HPLC. The quantity (Q) of the template bound to MIM3 or NIMs was calculated according to the following equation:

$$Q = \frac{(C_0 - C_t) \times V}{W}$$

where $C_0$ and $C_t$ (mg/L) are the initial concentration and the residual concentration of (S)-ketoprofen, respectively; $V$ (L) is the initial volume of the solution, and $W$ (g) is the weight of the MIM3 or NIMs. The imprinting factor ($\alpha$) was used to evaluate the specific recognition property of MIM3. This was defined as

$$\alpha = \frac{Q_{\text{MIM3}}}{Q_{\text{NIMs}}}$$

where $Q_{\text{MIM3}}$ and $Q_{\text{NIMs}}$ are the quantities of (S)-ketoprofen adsorbed on MIM3 and NIMs, respectively.

## 3. Results and discussion

### 3.1. Characteristics of MIMs

#### 3.1.1. FT-IR spectra

FT-IR spectra of activated silica microspheres, vinylated silica microspheres and MIM3 are shown in Fig. 3. The C=O stretch, C=C stretch and the saturated C–H peak of MPTS were 1723, 1638 and 2958 $cm^{-1}$, respectively (Fig. 3b). These new bands were attributed

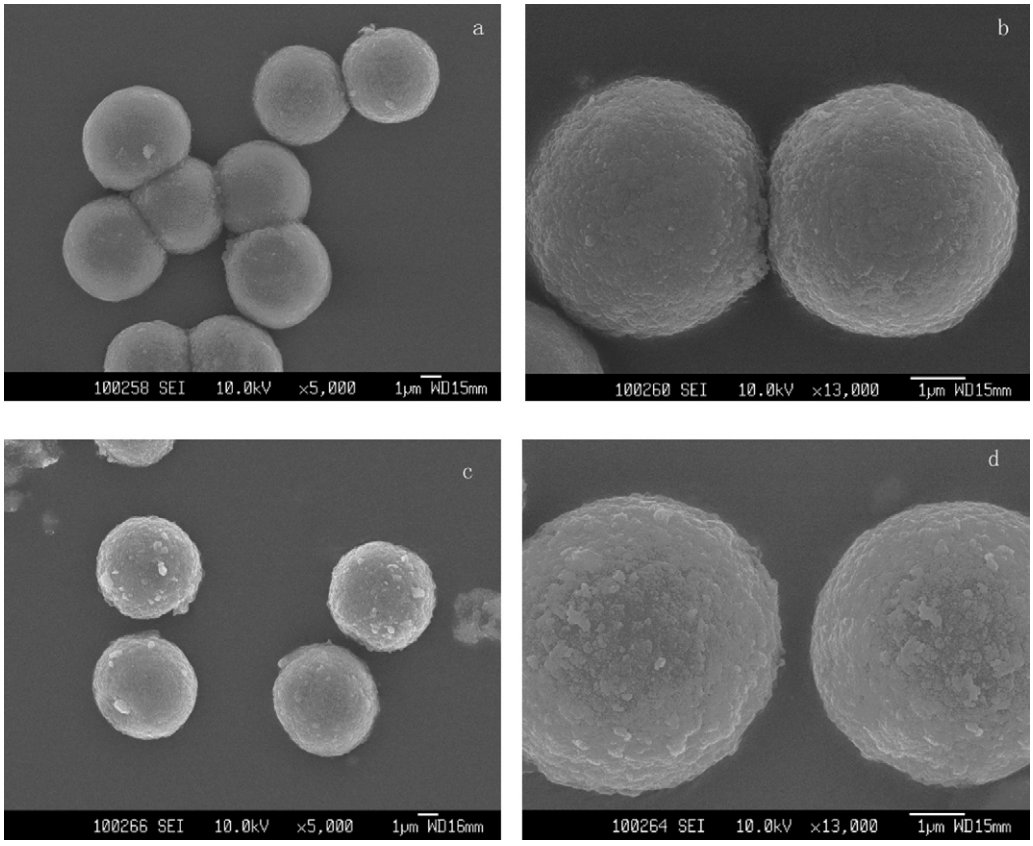


**Fig. 4.** SEM images of activated silica microspheres (magnification: (a) 5000× and (b) 13,000×) and MIM3 (magnification: (c) 5000× and (d) 13,000×).

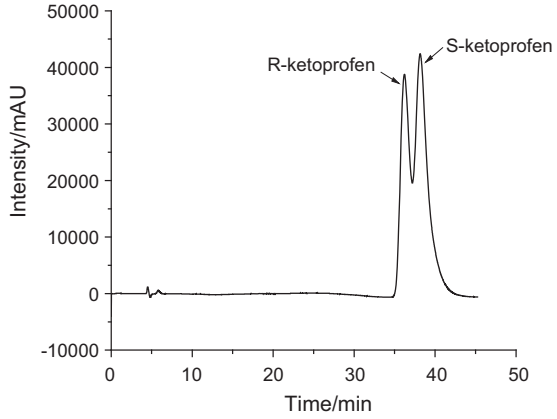


**Fig. 5.** Chromatogram of rac-ketoprofen on NIMs.

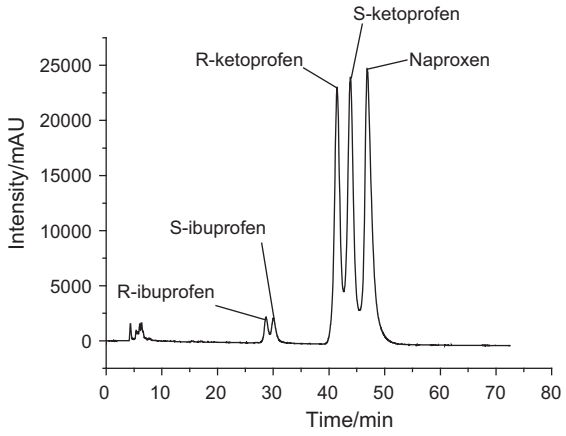


**Fig. 6.** Chromatogram of three non-steroidal anti-inflammatory drugs on MIM3.

to the fact that MPTS had been modified on the surface of silica microspheres. Successful preparation of MIM3 was judged by the peak of the skeleton vibration at 1645 and 1430 $cm^{-1}$ and C–H bending vibration at 741 and 703 $cm^{-1}$, which can be attributed to the quinoline ring (Fig. 3c).

### 3.1.2. SEM

The morphology of the activated silica microspheres and MIM3 is shown in Fig. 4. It is clear that we obtain monodisperse and regularly shaped molecularly imprinted microspheres. In comparison with activated silica microspheres, the imprinted microspheres show changes in surface modification characteristics: the increase of average particle diameter and more roughness. The porous surface helps the target molecules' distribution and retention. This makes MIM3 suitable as chromatographic stationary phase for analysis and evaluation of various related adsorbents.

## 3.2. Chromatographic analysis

Molecularly imprinted polymers are usually evaluated as the HPLC stationary phase because of good reproducibility, high efficiency and sensitivity of the method. Thus, the MIMs obtained using our new method were packed into the HPLC column to study their specific absorption characteristics and recognition mechanisms.

### 3.2.1. Optimization of preparation condition

Once the chiral functional monomer has been selected, the choice of a single chiral template molecule is one of the most important factors in the construction of molecularly imprinted polymers with high enantioselectivity. In general, the longer the retention time for enantiomer used as the template molecule, the more effective are the MIPs for the purpose of chiral separation. The chiral separation results for rac-ketoprofen on the NIMs column are shown in Fig. 5. The NIMs have stronger adsorption for (S)-ketoprofen than for (R)-ketoprofen, which indicates that (S)-ketoprofen matches the chirality of the allylcarbamate-cinchonine ester better than (R)-ketoprofen. Therefore, we used (S)-ketoprofen as the template to enhance the enantioselectivity of MIMs.

After functional monomer, cross-linker and template are chosen, the best conditions for MIPs formation can be determined only by empirical optimization, involving synthesis and evaluation of several polymers. This process is very time-consuming [40]. We have designed a single monomer which eliminates variables such as choice of the ratio of functional monomer to cross-linker and the ratio of functional monomer to template, which normally complicate MIPs' design. The synthesis of various MIMs was performed only to optimize the ratio of chiral monomer to template, which made the molecular imprinting process easier. The conditions used are shown in Table 1. The resolution of ketoprofen on the MIM1, MIM2, MIM3, MIM4 and MIM5 columns were 1.06, 1.17, 1.25, 1.21 and 1.00, respectively. MIM3 shows higher resolution than other molecularly imprinted polymers examined here.

### 3.2.2. pH effect on the chiral separation

Acetic acid in mobile phase can promote ion-pairing interactions between analyte and stationary phase. The retention time of (S)-ketoprofen on MIM3 column was increased by lowering pH of the mobile phase from 6.0 to 3.5. Cinchonine is a basic compound with complex multi-ring structure, a diprotic, ionizable weak base containing two basic nitrogen atoms with p*K*a1 and p*K*a2 values around 4.3 and 8.5, respectively. We believe that one of the most important factors in chiral separation on MIM3 column is ion-pairing between ketoprofen and the stationary phase. When the amount of acetic acid is increased, tertiary amine of allylcarbamate-cinchonine ester combines one $H^+$ to form a quaternary ammonium cation; as a result, there are more binding sites, enhancing the interaction between carboxyl anion of ketoprofen and the stationary phase. Thus, a good separation of ketoprofen on the MIM3 column can be achieved.

### 3.2.3. Synergistic effect in the chiral separation

The separation characteristics of NIMs and MIM3 columns were compared under optimized chromatographic conditions. As shown in Figs. 5 and 6, the resolution values for ketoprofen on NIMs and MIM3 were 0.62 and 1.25, respectively. The experiments confirmed our original hypothesis of synergistic effect in the chiral separation

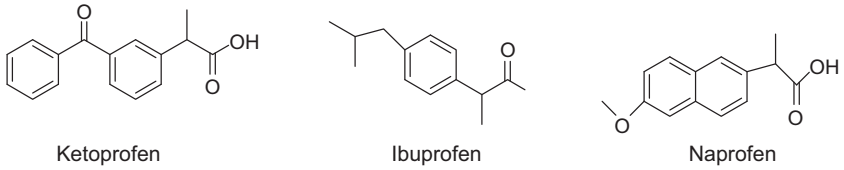


**Fig. 7.** The structures of ketoprofen, ibuprofen, and naproxen.

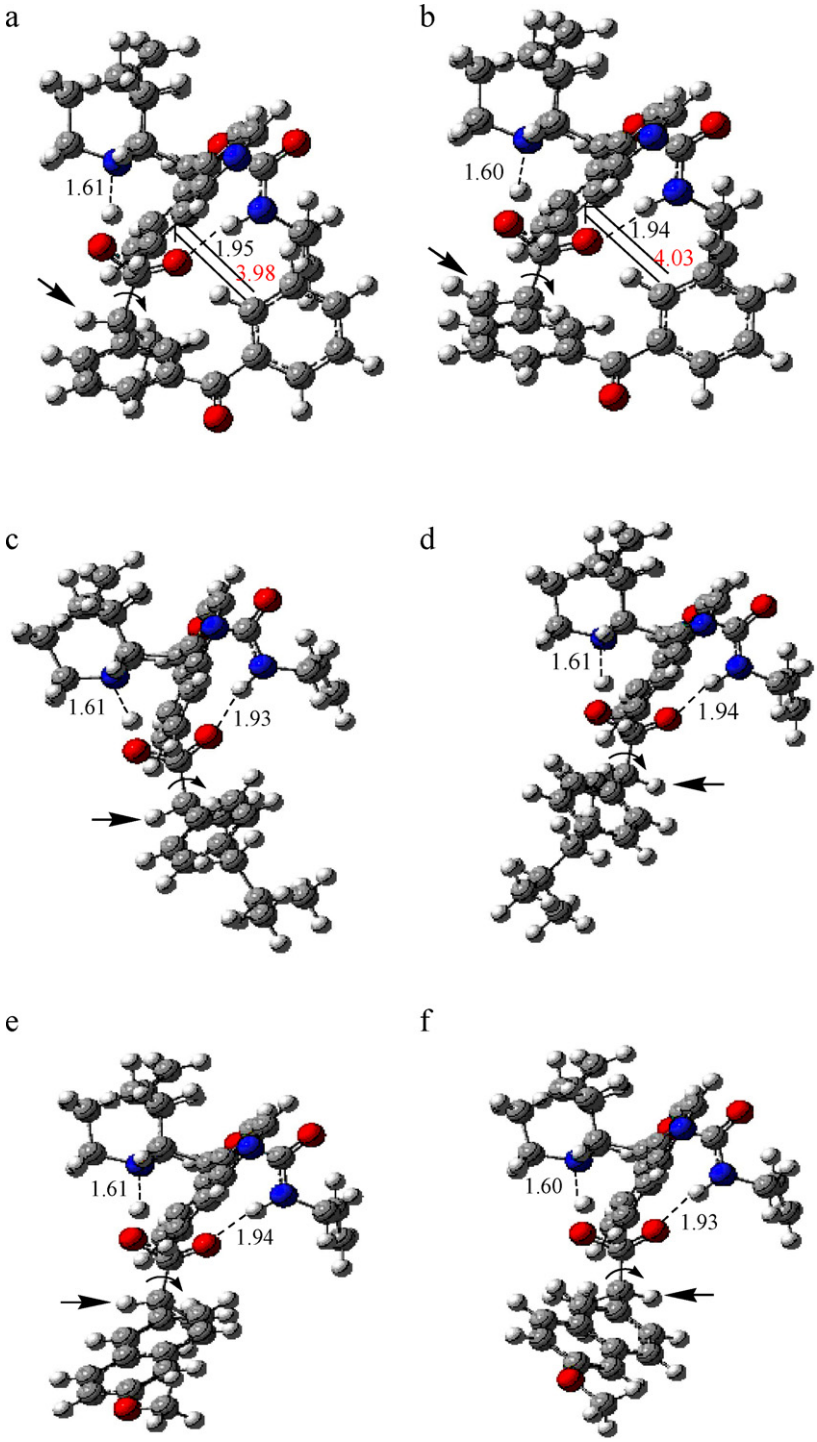


**Fig. 8.** Optimized structures of pre-arrangement between chiral monomer(ACC) and template or its analogues (distance in Å):(a) (S)-KEP; (b) (R)-KEP; (c) (S)-IBU; (d) (R)-IBU; (e) (S)-NAP; (f) (R)-NAP.

process on materials prepared using a chiral monomer and optical isomer templates.

### 3.2.4. Chiral recognition mechanism

(S)-ketoprofen templates were extracted from MIM3 to generate target-specific binding cavities, complementary to the single optical isomer in size, shape and functional groups. The imprinted cavities were more suitable for (S)-ketoprofen than (R)-ketoprofen, which was reflected in the retention time of (R)-ketoprofen—shorter than that of (S)-ketoprofen.

**Table 2**
The binding energy between chiral monomer (ACC) and template molecule or its analogues.

| Binding energy *E* (Kcal/mol) | | | | |
|---|---|---|---|---|
| | S-configuration | | R-configuration | |
| | Vacuum | $CHCl_3$ | Vacuum | $CHCl_3$ |
| KEP | −18.7 | −12.8 | −17.6 | −10.5 |
| IBU | −17.4 | −11.3 | −16.8 | −10.5 |
| NAP | −17.6 | −11.5 | −16.7 | −10.2 |

To investigate further the π–π interaction between host and guest, we synthesized allylcarbamate-quinidine ester and prepared MIM5 column. The resolution of ketoprofen on MIM5 was only 1.00, lower than that on MIM3, which might be attributed to the π–π interaction between the phenyl ring of ketoprofen and MIM5's quinoline ring with methoxyl group. Compared with MIM3, the quinoline ring of MIM5 has a lower electron density due to an extra electron-withdrawing substituent (methoxyl group) in MIM5, thus the π–π interaction between the ketoprofen and the MIM3 is a stronger than that between the ketoprofen and the MIM5, which could increase the chiral selectivity and the retention time of ketoprofen. This suggests that π–π interactions play an important role in the enantioseparation process of ketoprofen on MIM columns.

Two other non-steroidal anti-inflammatory drugs, structural analogues of ketoprofen, were selected to investigate the chiral recognition mechanism of the MIMs. The racemic mixture of ibuprofen, ketoprofen, and naproxen (Fig. 7) was separated on MIM3 column under optimized conditions. The result is shown in Fig. 6. Rac-ketoprofen had the best resolution; the resolution of rac-ibuprofen was 0.87, but rac-naproxen could not be enantioseparated.

The imprinted cavity is large enough for the smaller ibuprofen to enter. The π–π interaction between ibuprofen and MIM3 is weaker than that between ketoprofen and MIM3 because ibuprofen molecule lacks the terminal phenyl ring. As a result, ibuprofen has lower chiral resolution; its retention time on MIM3 column is shorter than ketoprofen's. The chirality of imprinted cavities were matching (S)-ibuprofen rather than (R)-ibuprofen, resulting in (S)-ibuprofen's longer retention time. The retention time of naproxen was longer than that of ketoprofen, which might be related to its stronger hydrophobicity. However, naproxen molecule is bigger than ketoprofen, resulting in size-exclusion effect. Therefore, rac-naproxen could not been enantioseparated on MIM3 column.

To achieve chiral recognition, there should be at least three interactions between chiral stationary phase and raceme [41]. The chromatographic data from our work suggest that five different factors contribute to the chiral recognition of rac-ketoprofen on MIM3: (1) the size and shape of the imprinted cavity; (2) matching the chirality of the chiral monomer and (S)-ketoprofen; (3) the π–π interactions between MIM3 and (S)-ketoprofen;(4) the hydrogen-bonding between the secondary amine group in MIM3 and the carbonyl in (S)-ketoprofen; (5) the ion-pair interactions between the tertiary amine cation in host and the carboxyl anion in (S)-ketoprofen.

### 3.3. Computational simulation

The binding energies of complex with KEP, NAP, and IBU are listed in Table 2. A lower the binding energy indicates a stronger the pre-arrangement and a better the molecular recognition capacity. The results show that the pre-arrangement of complex with KEP is stronger than that with IBU and NAP. From the optimized structures (Fig. 8), it is found that the carboxyl group can form an ion-pair with the tertiary amine of the monomer about 1.60 Å away and a hydrogen bond with the amide about 1.93 Å away. But for KEP, there is an extra π–π interaction [42] between the terminal phenyl ring of KEP and the quinolyl ring of chiral monomer. So, the pre-arrangement of complex with KEP is stronger than that with IBU and NAP. Comparing the bind energies between the complex with S- and R-enantiomer of KEP, NAP and IUB, it is found that recognition is more favorable for the S-enantiomer. Thus, recognition is part of the chiral-matching process, and the chirality of template molecules affects the recognition selectivity. Moreover, the chiral recognition selectivity of KEP is better than that of IBU and NAP (see Table 2). The optimized structures show that internal phenyl ring is eclipsed by a C–H bond in complex with (S)-KEP, but eclipsed by a C–C bond in complex with (R)-KEP (shown in Fig. 8). To maintain the π–π interaction, the internal phenyl ring of (R)-KEP cannot rotate to a more sterically favored configuration, which results in higher binding energy difference (1.1 Kcal/mol in vacuum and 2.0 Kcal/mol in $CHCl_3$, respectively) between complex with (S)-KEP and (R)-KEP. For IBU and NAP, the phenyl ring or naphthyl ring is always eclipsed by C–H bond because there is no π–π interaction to confine the C–C bond rotation. Therefore, the energy difference between complex with S- and R-enantiomer of NAP and IBU is low (less than 1 Kcal/mol in vacuum and 1.3 Kcal/mol in $CHCl_3$, respectively). These results show that the extra π–π interaction of KEP results in stronger pre-arrangement and better chiral recognition selectivity. However, the chiral recognition of MIPs is determined not only by the magnitude of pre-arrangement, but also by the properties of recognition site, such as shape, size, etc. KEP had the largest bind energy difference between complex with S- and R-enantiomer. Therefore, it had the best chiral recognition selectivity of the three molecules considered. However, NAP had larger energy difference than IBU. But there is almost no recognition selectivity for NAP. The size of naphthyl ring of NAP is too large to contribute to the recognition site formed by phenyl ring of KEP in pre-arrangement of complex with KEP.

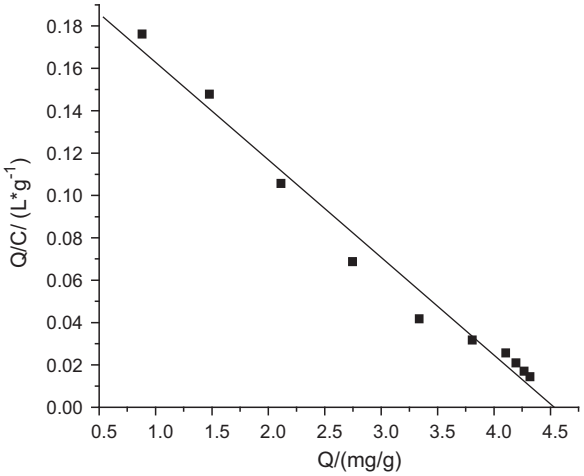


**Fig. 9.** Scatchard plot of the experimental adsorption isotherm for MIM3.

### 3.4. Binding characteristics

To evaluate the binding parameters, we performed an equilibrium adsorption experiment with MIM3 and NIMs. The adsorption capacity of (S)-keteprofen on MIM3 and NIMs increases with its growing initial concentration. The saturated adsorption capacity for MIM3 was 4.319 mg/g and only 1.247 mg/g for NIM, giving the imprinting factor ($\alpha$) of 3.46. To see multiple classes of binding sites, the data were further processed using Scatchard analysis [43], replotting the binding isotherm in the format of $Q/C_{(S)\text{-keteprofen}}$ versus $Q$ (Fig. 9). The equilibrium dissociation constant ($K$) and the apparent maximum number of binding sites ($Q_{max}$) can be calculated according to the slopes and intercepts in the linear Scatchard analysis. The Scatchard plot for MIM3 was virtually linear, which suggests that MIM3 contains only a homogeneous population of binding sites with specific adsorption for (S)-keteprofen. The $K$ and $Q_{max}$ values were 0.085 mmol/L and 4.54 mg/g, respectively.

## 4. Conclusions

We developed a systematic method for molecular imprinting process, taking advantage of the synergistic effect in the chiral

separation. The imprinted microspheres obtained using our procedure possessed both the characteristics of brush-type chiral stationary phases and of common MIPs based on chiral three-dimensional cavities. They exhibited a significant synergistic effect in enantioselective recognition. This was the result of matching chirality of the template molecule and the functional monomer, allylcarbamate-cinchonine ester, which was also employed as cross-linker. This chiral monomer has multi-binding sites for the template (S)-ketoprofen. We believe that the specific recognition of (S)-ketoprofen on MIM3 is related to the ion-pair interactions, hydrogen-bonding and the $\pi$–$\pi$ interactions between host and guest. The $\pi$–$\pi$ interactions play an important role in the chiral recognition process, affecting the separation efficiency. The results of the computational simulation support our hypothetical mechanism.

An additional benefit of the single monomer strategy is a considerable simplification of the MIMs preparation, making the process of the molecular imprinting a much more practical, easy to perform procedure. In comparison with the previous chromatogram of molecular imprinting, our chromatogram of MIM3 column show better enantiomer separation, with higher efficiency and good peak symmetry. We believe that this type of column is a promising tool for detection and separation of ketoprofen isomers or other non-steroidal anti-inflammatory drugs in aqueous media.

## Acknowledgement

This work is supported by the National Natural Science Foundation of China (No: 20875034).

## References

[1] H. Asanuma, T. Hishiya, M. Komiyama, Adv. Mater. 12 (2000) 1019.
[2] K. Yano, T. Nakagiri, T. Takeuchi, J. Matsui, K. Ikebukuro, I. Karube, Anal. Chim. Acta 357 (1997) 91.
[3] X.W. Kan, Z.R. Geng, Y. Zhao, Z.L. Wang, J.J. Zhu, Nanotechnology 20 (2009) 165601.
[4] R. Suedee, T. Srichana, T. Rattananont, Drug Deliv. 9 (2002) 19.
[5] R. Suedee, T. Srichana, R. Chotivatesin, G.P. Martin, Drug Dev. Ind. Pharm. 28 (2002) 545.
[6] D. Cunliffe, A. Kirby, C. Alexander, Adv. Drug Deliv. Rev. 57 (2005) 1836.
[7] M. Ali, M.E. Byrne, Pharm. Res. 26 (2009) 714.
[8] Z.X. Xu, G.Z. Fang, S. Wang, Food Chem. 119 (2010) 845.
[9] K. Adbo, I.A. Nicholls, Anal. Chim. Acta 435 (2001) 115.
[10] L. Ye, O. Ramström, K. Mosbach, Anal. Chem. 70 (1998) 2789.
[11] Y. Yu, L. Ye, V. de Biasi, K. Mosbach, Biotechnol. Bioeng. 79 (2002) 23.
[12] M. Javanbakht, M.H. Namjumanesh, B. Akbari-adergani, Talanta 80 (2009) 133.
[13] X.J. Liu, J.Z. Liu, Y.Y. Huang, R. Zhao, G.Q. Liu, Y. Chen, J. Chromatogr. A 1216 (2009) 7533.
[14] J.J. Ou, L. Kong, C.S. Pan, X.Y. Su, X.Y. Lei, H.F. Zou, J. Chromatogr. A 1117 (2006) 163.
[15] M. Jiang, Y. Shi, R.L. Zhang, C.H. Shi, Y. Peng, Z. Huang, B. Lu, J. Sep. Sci. 32 (2009) 3256.
[16] L.D. Yao, Y.W. Tang, W.P. Zeng, Z.F. Huang, Anal. Sci. 25 (2009) 1089.
[17] T. Alizadeh, M.R. Ganjali, P. Norouzi, M. Zare, A. Zeraatkar, Talanta 79 (2009) 1197.
[18] G.M. Birnbaumer, P.A. Lieberzeit, L. Richter, R. Schirhagl, M. Milnera, F.L. Dickert, A. Bailey, P. Ertl, Lab Chip 9 (2009) 3549.
[19] P. Pasetto, S.C. Maddock, M. Resmini, Anal. Chim. Acta 542 (2009) 66.
[20] B.P. Santora, A.O. Larsen, M.R. Gagné, Organometallics 17 (1998) 3138.
[21] B. Sellergren, M. Lepistö, K. Mosbach, J. Am. Chem. Soc. 110 (1988) 5853.
[22] M. Kempe, L. Fischer, K. Mosbach, J. Mol. Recognit. 6 (1993) 25.
[23] M. Kempe, Anal. Chem. 68 (1996) 1948.
[24] Z. Lian, F. Yang, X.W. He, X.M. Zhao, Y.K. Zhang, J. Chromatogr. A 1216 (2009) 8612.
[25] O. Ramström, I.A. Nicholls, K. Mosbach, Tetrahedron:Asymmetry 5 (1994) 649.
[26] S.A. Piletsky, E.V. Piletska, K. Karim, K.W. Freebaim, C.H. Legge, A.P.F. Turner, Macromolecules 35 (2002) 7499.
[27] N.M. Maier, W. Lindner, Anal. Bioanal. Chem. 389 (2007) 377.
[28] R.J. Ansell, Adv. Drug Deliv. Rev. 57 (2005) 1809.
[29] A. Kugimiya, T. Takeuchi, Anal. Chim. Acta 395 (1999) 251.
[30] E. Gavioli, N.M. Maier, K. Haupt, K. Mosbach, W. Lindner, Anal. Chem. 77 (2005) 5009.
[31] J.J. Kirkland, Completely porous microspheres for chromatographic uses, US Patent 3,782,075 (1974).
[32] D.M. Han, G.Z. Fang, X.P. Yan, J. Chromatogr. A 1100 (2005) 131.
[33] M. Lämmerhofer, W. Lindner, J. Chromatogr. A 741 (1996) 33.
[34] M.J. Frisch, et al., Gaussian 03, Revision E. 01, Gaussian, Inc., Wallingford, CT, 2004.
[35] A.D. Becke, J. Chem. Phys. 98 (1993) 5648.
[36] C. Lee, W. Yang, G. Parr, Phys. Rev. B 37 (1988) 785.
[37] M.T. Cances, B. Mennucci, J. Tomasi, J. Chem. Phys. 107 (1997) 3032.
[38] M. Cossi, V. Barone, B. Mennucci, J. Tomasi, Chem. Phys. Lett. 286 (1998) 253.
[39] B. Mennucci, J. Tomasi, J. Chem. Phys. 106 (1997) 5151.
[40] M. Sibrian-Vazquez, D.M. Spivak, J. Am. Chem. Soc. 126 (2004) 7827.
[41] V.A. Davankov, Chirality 9 (1997) 99.
[42] M.O. Sinnokrot, E.F. Valeev, C.D. Sherrill, J. Am. Chem. Soc. 124 (2002) 10887.
[43] J.A. García-Calzón, M.E. Díaz-García, Sens. Actuators B 123 (2007) 1180.